Journal of Applied Fluid Mechanics, Vol. 8, No. 2, pp. 189-196, 2015.
Available online at www.jafmonline.net, ISSN 1735-3572, EISSN 1735-3645.
DOI: 10.18869/acadpub.jafm.67.221.19377

Magnetic Field Effect on Natural Convection Flow with Internal Heat Generation using Fast Ψ – Ω Method

M. A. Taghikhani

Department of Engineering, Imam Khomeini International University, Qazvin, Iran

Corresponding Author Email: taghikhani@ENG.ikiu.ac.ir

(Received Sep 20, 2012; accepted May 21, 2014)

ABSTRACT

The magnetic field effect on laminar natural convection flow is investigated in a filled enclosure with internal heat generation using two-dimensional numerical simulation. The enclosure is heated by a uniform volumetric heat density and walls have constant temperature. A fixed magnetic field is applied to the enclosure. The dimensionless governing equations are solved numerically for the stream function, vorticity and temperature using finite difference method for various Rayleigh (*Ra*) and Hartmann (*Ha*) numbers in MATLAB software. The stream function equation is solved using fast Poisson's equation solver on a rectangular grid (POICALC function in MATLAB), voricity and temperature equations are solved using red-black Gauss-Seidel and bi-conjugate gradient stabilized (BiCGSTAB) methods respectively. The results show that the strength of the magnetic field has significant effects on the flow and temperature fields. For the square cavity, the maximum temperature reduces with increasing *Ra* number. It is also observed that at low *Ra* number, location of the maximum temperature is at the centre of the cavity and it shifts upwards with increase in *Ra* number. Circulation inside the enclosure and therefore the convection becomes stronger as the *Ra* number increases while the magnetic field suppresses the convective flow and the heat transfer rate. The ratio of the Lorentz force to the buoyancy force (Ha^2/Ra) is as an index to compare the contribution of natural convection and magnetic field strength on heat transfer.

Keywords: Magnetohydrodynamics (MHD), Natural convection, Square cavity, Stream function, Vorticity, Poicalc function.

NOMENCLATURE

B magnetic flux density vector: $Wb \cdot m^{-2}$
C_p specific heat: $J.kg^{-1}.K^{-1}$
g gravitational acceleration vector: $m \cdot s^{-2}$
h grid spacing: m
J electric current density vector: $A \cdot m^{-2}$
k thermal conductivity: $W \cdot m^{-1} \cdot K^{-1}$
L dimension of cavity: m
p pressure: $N \cdot m^{-2}$
q volumetric heat source density: $W.m^{-3}$
T temperature: K
v velocity vector: $m \cdot s^{-1}$
x, y, z Cartesian coordinates: m

Greek symbols

α thermal diffusivity: $m^2 \cdot s^{-1}$
β coefficient of volumetric expansion: K^{-1}
φ electric potential: V
μ dynamic viscosity: $kg.\ m^{-1}.s^{-1}$
ρ density: $kg.m^{-3}$
σ electrical conductivity: $mho.m^{-1}$
ω vorticity: s^{-1}
Ψ stream function: $m^2.s^{-1}$

Subscript

0 reference value
max maximum value
x, y, z component of a vector quantity

Dimensionless quantities

V velocity vector
X Cartesian coordinate in x direction
Y Cartesian coordinate in y direction
Ω vorticity
Ψ stream function
θ temperature

Dimensionless numbers

Gr Grashof number
Ha Hartmann number
Pr Prandtl number
Ra *Rayleigh number*

1. INTRODUCTION

The set of equations which describe MHD are a combination of the Navier-Stokes equations of fluid dynamics and Maxwell's equations of electromagnetism. These differential equations are solved simultaneously, either analytically or numerically. In industrial problems and microelectronic heat transfer devices flow of an electrically conducting fluid subjected to a magnetic field is used, thus, the fluid experiences a Lorentz force and its effect is to reduce the flow velocities which turn the affects in the heat transfer rate. Laminar natural convection flows have significant applications in many engineering areas including cooling of electronic equipment, nuclear reactor insulation, solar energy collection, and crystal growth in liquids and have been investigated by a number of researchers and a rich and variety of numerical results have been published due to this phenomenon.

An analytical solution to the equations of magnetohydrodynamic flow is proposed in (Garandet and Alboussiere, 1992) and is used to model the effect of a transverse magnetic field on buoyancy driven convection in a two-dimensional cavity. The control volume algorithm is used in (Al-Najem et al., 1998; Sarris et al., 2005; Kandaswamy et al., 2008; Sheikhzadeh et al., 2011) to solve the two dimensional transient MHD equations with alternating direct implicit procedure (ADI). Finite difference method and finite element method are developed in (Borghi et al., 1996; Borghi et al., 2004; Verardi and Cardoso 1998; Verardi et al., 2001; Verardi et al., 2002; Shadid et al., 2010) for the solution of two-dimensional steady state electrodynamic problem in magnetohydrodynamic flows. A mathematical model describing the dynamics of magnetic field influence on a conducting liquid in a square cavity is presented in (Krzeminski et al., 2000) such that biharmonic mathematical model is used with stream function and the magnetic potential.

A finite element method for the solution of 3D incompressible magnetohydrodynamic flow is presented in (Salah et al., 2001). The buoyancy-driven magnetohydrodynamic flow in a liquid-metal filled cubic enclosure with internal heat generation is investigated by three-dimensional numerical simulation in (Piazza and Ciofalo, 2002). Reference (Mahmud et al., 2003) has performed an analysis to study the first and second laws (of thermodynamics) characteristics of flow and heat transfer inside a vertical channel made of two parallel plates under the action of transverse magnetic field. A two-dimensional mathematical model has been developed to study the interaction between gravitational body force and self-induced electromagnetic body force in a Joule-heated liquid pool in a rectangular cavity, with an aspect ratio of 2 in (Sugilal et al., 2005).

Steady, laminar, natural-convection flow in the presence of a magnetic field in an inclined rectangular enclosure heated from one side and cooled from the adjacent side is considered in (Ece and Büyük, 2006; Ece and Büyük 2007) so that the governing equations are solved numerically for the stream function, vorticity and temperature using the differential quadrature method. A finite volume code based on PATANKAR's SIMPLER method is utilized in (Pirmohammadi et al., 2009; Pirmohammadi and Ghassemi 2009; Pirmohammadi et al., 2010; Pirmohammadi et al., 2011) with constant Prandtl (*Pr*) number.

The present study investigates the laminar steady convection in an enclosure in the presence of a magnetic field. The enclosure is filled with an electrically conducting fluid whose Prandtl number is 0.733. Therefore, a two-dimensional numerical model is developed to solve the vorticity, stream function and temperature governing equations of buoyancy-driven natural convection flow inside a cavity. The study pursues numerical solution to study the effect of magnetic field strength and *Ra* number on the natural convection and heat transfer.

2. MATHEMATICAL FORMULATION

Steady, laminar, natural-convection flow is considered in the presence of a magnetic field in a square enclosure. Dimensional coordinates with the x-axis measuring along the bottom wall and y-axis being normal to it along the left wall are used. The geometry and the coordinate system are schematically shown in Fig. 1. Magnetic flux density *B* is applied with respect to the coordinate system. The walls are kept at a constant temperature T=0. (Bagewadi and Bhagya 2011; Kadid et al., 2011)

Continuity, change of linear momentum and energy equations are written as follows

$$\vec{\nabla}\cdot\vec{v}=0 \tag{1}$$

$$\rho\left(\vec{v}.\vec{\nabla}\right)\vec{v}=\rho\,\vec{g}-\vec{\nabla}p+\mu\nabla^2\vec{v}+\vec{J}\times\vec{B} \tag{2}$$

$$\left(\vec{v}.\vec{\nabla}\right)T=\alpha\nabla^2T+\frac{q}{\rho C_p} \tag{3}$$

where, $\vec{v}$ is the velocity vector, p is the pressure, T is the temperature, $\vec{g}$ is the gravitational acceleration, ρ is the density, μ is the viscosity, C_p is the specific heat, α is the thermal diffusivity of the fluid and q is volumetric heat density, respectively, $\vec{J}$ is the current density and $\vec{B}$ is magnetic field. The magnetic Reynolds number is small and the induced magnetic field due to the motion of the electrically conducting fluid is neglected. The current density is

$$\vec{J}=\sigma(-\vec{\nabla}\phi+\vec{v}\times\vec{B}) \tag{4}$$

Where σ is the electrical conductivity of the fluid and ϕ is the electric potential. The conservation of the electric charge is

$$\vec{\nabla}\cdot\vec{J}=0 \tag{5}$$

From (4) and (5) is derived:

$$\nabla^2\phi=0 \tag{6}$$

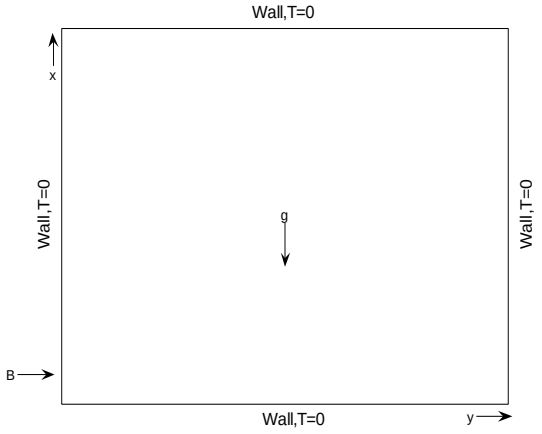

Fig. 1. Geometry and the coordinate system

Since there is always somewhere around the cavity an electrically insulating boundary, the unique solution is $\vec{\nabla}\phi = 0$ which means that the electric field vanishes everywhere. The governing equations in scalar form under Boussinesq approximation are written as

$$\frac{\partial v_x}{\partial x} + \frac{\partial v_y}{\partial y} = 0 \tag{7}$$

$$-\mu\left(\frac{\partial^2 v_x}{\partial x^2} + \frac{\partial^2 v_x}{\partial y^2}\right) + \rho_0\left(v_x\frac{\partial v_x}{\partial x} + v_y\frac{\partial v_x}{\partial y}\right) = -\frac{\partial p}{\partial x} \tag{8}$$

$$-\mu\left(\frac{\partial^2 v_y}{\partial x^2} + \frac{\partial^2 v_y}{\partial y^2}\right) + \rho_0\left(v_x\frac{\partial v_y}{\partial x} + v_y\frac{\partial v_y}{\partial y}\right) = -\frac{\partial p}{\partial y} - \rho_0(1-\beta T)g_y - \sigma B_x^2 v_y \tag{9}$$

$$-\alpha\left(\frac{\partial^2 T}{\partial x^2} + \frac{\partial^2 T}{\partial y^2}\right) + v_x\frac{\partial T}{\partial x} + v_y\frac{\partial T}{\partial y} = \frac{q}{\rho C_p} \tag{10}$$

Here β is the coefficient of thermal expansion of the fluid and ρ_0 is the density of the fluid at temperature $T=0$. Stream function and vorticity are defined as follows

$$v_x = \frac{\partial \psi}{\partial y} \tag{11}$$

$$v_y = -\frac{\partial \psi}{\partial x} \tag{12}$$

$$\omega = \frac{\partial v_y}{\partial x} - \frac{\partial v_x}{\partial y} \tag{13}$$

Therefore the governing equations reduce to

$$\frac{\partial^2 \psi}{\partial x^2} + \frac{\partial^2 \psi}{\partial y^2} = -\omega \tag{14}$$

$$\rho_0\left(v_x\frac{\partial \omega}{\partial x} + v_y\frac{\partial \omega}{\partial y}\right) = \mu\left(\frac{\partial^2 \omega}{\partial x^2} + \frac{\partial^2 \omega}{\partial y^2}\right) + \rho_0\beta g_y\frac{\partial T}{\partial x} - \sigma B_x^2\frac{\partial v_y}{\partial x} \tag{15}$$

Dimensionless variables used in the analysis are according to,

$$X = \frac{x}{L}\ ,Y = \frac{y}{L}\ ,V_x = \frac{Lv_x}{\alpha}\ ,V_y = \frac{Lv_y}{\alpha}\ ,$$

$$\boldsymbol{\Psi} = \frac{\psi}{\alpha}\ ,\boldsymbol{\Omega} = \frac{L^2\omega}{\alpha}\ ,\theta = \frac{k.T}{L^2 q} \tag{16}$$

where k is the thermal conductivity. Dimensionless numbers, the Prandtl, Grashof, Rayleigh and Hartmann numbers are defined as follows,

$$\mathrm{Pr} = \frac{\mu}{\rho_0\alpha}\ ,\ Gr = \frac{\rho_0^2 g_y \beta L^5 q}{k\mu^2}\ ,$$

$$Ra = \mathrm{Pr}.Gr\ ,Ha = BL\sqrt{\frac{\sigma}{\mu}} \tag{17}$$

According to the equations (16) and (17), the governing equations in this study are given in dimensionless form as

$$\frac{\partial^2 \boldsymbol{\Psi}}{\partial X^2} + \frac{\partial^2 \boldsymbol{\Psi}}{\partial Y^2} = -\boldsymbol{\Omega} \tag{18}$$

$$(V_x\frac{\partial \boldsymbol{\Omega}}{\partial X} + V_y\frac{\partial \boldsymbol{\Omega}}{\partial Y}) = \mathrm{Pr}(\frac{\partial^2 \boldsymbol{\Omega}}{\partial X^2} + \frac{\partial^2 \boldsymbol{\Omega}}{\partial Y^2}) + \mathrm{Pr}\,Ra\frac{\partial \theta}{\partial X} - \mathrm{Pr}\,Ha^2\frac{\partial V_y}{\partial X} \tag{19}$$

$$V_x\frac{\partial \theta}{\partial X} + V_y\frac{\partial \theta}{\partial Y} = (\frac{\partial^2 \theta}{\partial X^2} + \frac{\partial^2 \theta}{\partial Y^2}) + 1 \tag{20}$$

Which these equations are solved subject to the boundary conditions $\boldsymbol{\Psi} = 0$ and $\theta = 0$ at all walls. The vorticity values at the wall is calculated using Jensen's formula (Erturk, 2009)

$$\boldsymbol{\Omega}_0 = \frac{-4\boldsymbol{\Psi}_1 + 0.5\boldsymbol{\Psi}_2}{h^2} - \frac{3V}{h} \tag{21}$$

Where subscript 0 refers to the points on the wall, 1 refers to the points adjacent to the wall, 2 refers to the second line of points adjacent to the wall, *V* refers to the velocity of the wall with its value being equal to 1 on the moving wall, and 0 on the stationary walls while *h* is the grid spacing. The velocities at a point (x,y) are approximated as follow (Gupta and Kalita, 2005):

$$V_x(x,y) = \frac{3}{4h}[\boldsymbol{\Psi}(x,y+h) - \boldsymbol{\Psi}(x,y-h)] - \frac{1}{4}[V_x(x,y+h) - V_x(x,y-h)]$$

$$V_y(x,y) = -\frac{3}{4h}[\boldsymbol{\Psi}(x+h,y) - \boldsymbol{\Psi}(x-h,y)] - \frac{1}{4}[V_y(x+h,y) - V_y(x-h,y)] \tag{22}$$

3. SOLUTION METHOD

The dimensionless governing equations associated with the boundary conditions are solved for stream function, vorticity and temperature numerically using the second order finite difference method. The hybrid-scheme, which is a combination of the central difference scheme and the upwind scheme, is used to discretize the convection terms. The sequence of algorithm is provided here:

1. Guess the velocity and the stream function fields.

2. Solve discretized temperature equation using Jacobi BiCGSTAB method.

3. Calculate velocity field using stream function field (equation 22).

4. Calculate vorticity boundary condition using velocity and stream function fields (equation 21).

5. Solve the discretized vorticity equation using red-black Gauss-Seidel method.

6. Solve the discretized stream function equation using fast Poisson's equation solver on a rectangular grid (POICALC function) in MATLAB.

7. Check error in temperature, vorticitty and stream function fields. If errors are below the specified tolerance then exit the loop otherwise relax variables and return to step 2. Repeat the whole procedure till converged solution is obtained. The tolerance of the convergence criterion used for all variables is 10^{-6}:

$$\left|\frac{\theta^{k+1}-\theta^{k}}{\theta^{k+1}}\right| \le 10^{-6} \tag{23}$$

$$\left|\frac{\Psi^{k+1}-\Psi^{k}}{\Psi^{k+1}}\right| \le 10^{-6} \tag{24}$$

$$\left|\frac{\Omega^{k+1}-\Omega^{k}}{\Omega^{k+1}}\right| \le 10^{-6} \tag{25}$$

3.1. Grid Refinement Check

In order to determine the proper grid size for this study, a grid independence test are conducted with Pr=1 and Ra=10^5. The following six grid sizes are considered for the grid independence study. These grid densities are 32×32, 40×40, 64×64, 80×80, 96×96 and 128×128. The maximum temperature θ_{max} and maximum stream function Ψ_{max} of the fluid in the cavity are used as a sensitivity measure of the accuracy of the solution and are selected as the monitoring variables for the grid independence study. Table 1 shows the dependence of the quantities θ_{max} and Ψ_{max} on the grid size. Considering the accuracy of the numerical values, the following calculations are performed with 64×64 grid.

Table 1 Grid sensitivity check at Pr=1 and Ra=10^5

Grid size	Ha=0		Ha=100	
	θ_{max}	Ψ_{max}	θ_{max}	Ψ_{max}
32×32	0.064688	2.3540	0.073602	0.044403
40×40	0.064730	2.3493	0.073623	0.043853
64×64	0.064727	2.3423	0.073645	0.043171
80×80	0.064714	2.3419	0.073651	0.043056
96×96	0.064718	2.3409	0.073653	0.042970
128×128	0.064717	2.3390	0.073661	0.042910

3.2. Code Validation

In order to verify the accuracy of the numerical code, comparisons with the previously published results are necessary. The present numerical code is verified against a documented numerical study. The code is benchmarked with a differentially heated cavity problem, witch the right wall maintained at cooled condition. The left wall is hot whereas the two horizontal walls are under adiabatic condition. The governing equations are solved on a uniform grid of 64×64, and for a Prandtl number, Pr = 0.733. The solutions are obtained for two values of Rayleigh number 10^4, 10^5 and Hartmann number Ha=0. The Pr and Ra are chosen such that the direct comparison to be possible with the benchmark solution (Pirmohammadi et al., 2009) which is based on finite volume scheme. The isotherms and streamlines are compared with results of (Pirmohammadi et al., 2009) in figures 2 and 3. It is observed that the present results agree well with previous numerical work.

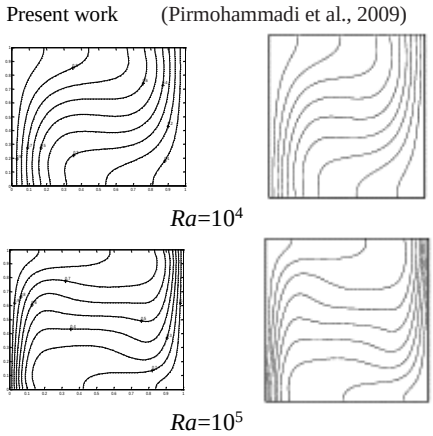

Fig. 2. Comparison of isotherms at various Ra and Ha=0

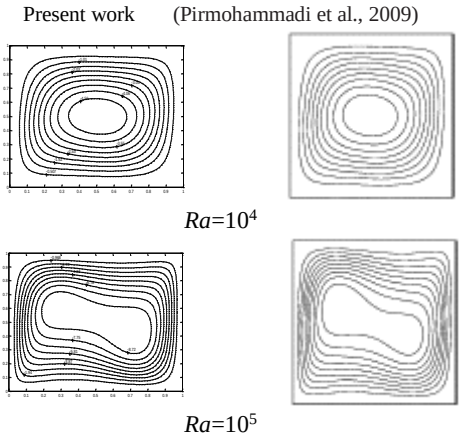

Fig. 3. Comparison of streamlines at various Ra and Ha=0

4. RESULTS AND DISCUSSIONS

Parametric investigations are performed for a square cavity in the following range of parameter values:

Rayleigh number: $10^4 \le Ra \le 10^7$;

Prandtl number: Pr=0.733;

Hartmann number: $0 \le Ha \le 500$.

The influence of the Ha number on the streamlines and isotherms inside the cavity at Ra=10^6 are shown in figures 4 - 15. Table2 shows variations of dimensionless maximum temperature (θ_{max}) and dimensionless maximum stream function (Ψ_{max}) with Ha and Ra numbers. The maximum

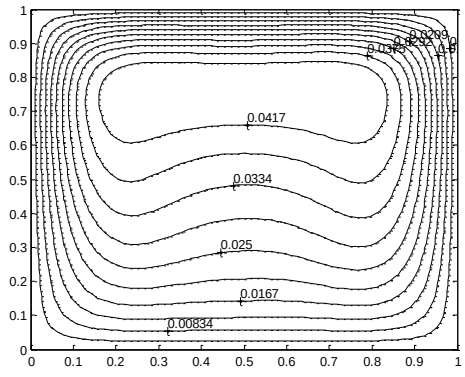

Fig .4. Isotherms of natural convection in a square cavity for $Ra=10^6$ and $Ha=0$

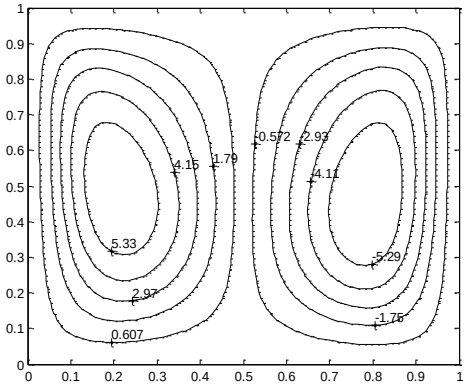

Fig. 5. Streamlines of natural convection in a square cavity for $Ra=10^6$ and $Ha=0$

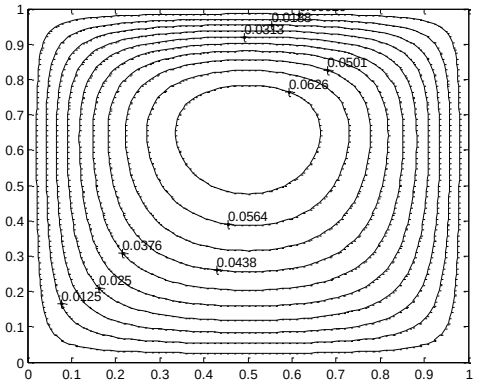

Fig. 6. Isotherms of natural convection in a square cavity for $Ra=10^6$ and $Ha=50$

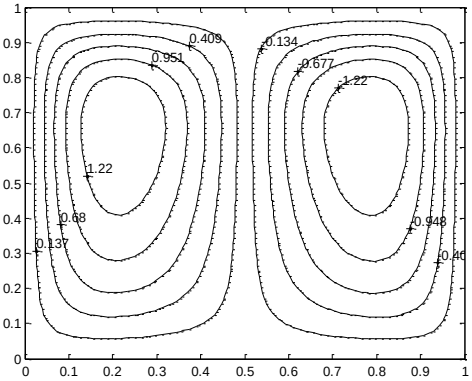

Fig. 7. Streamlines of natural convection in a square cavity for $Ra=10^6$ and $Ha=50$

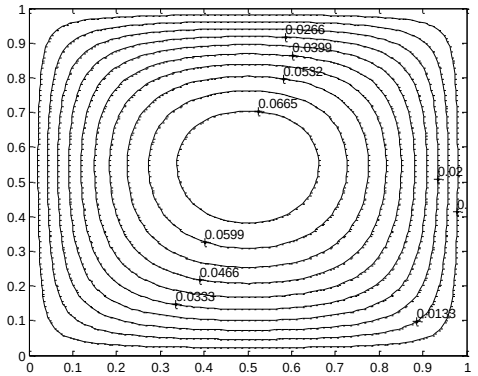

Fig. 8. Isotherms of natural convection in a square cavity for $Ra=10^6$ and $Ha=100$

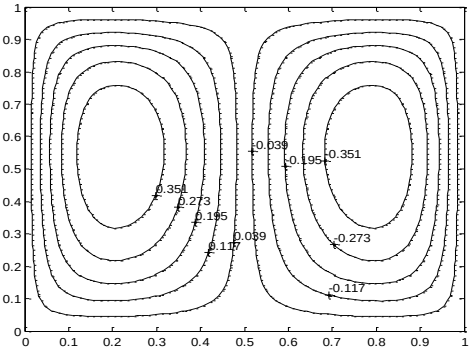

Fig. 9. Streamlines of natural convection in a square cavity for $Ra=10^6$ and $Ha=100$

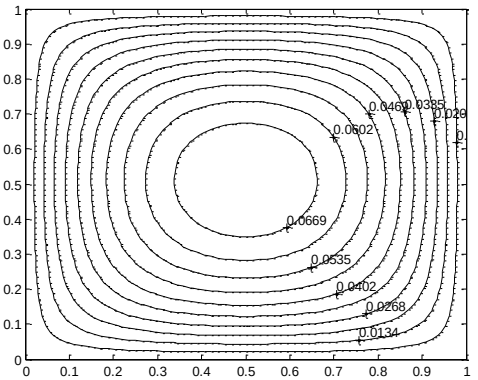

Fig.10.Isotherms of natural convection in a square cavity for $Ra=10^6$ and $Ha=200$

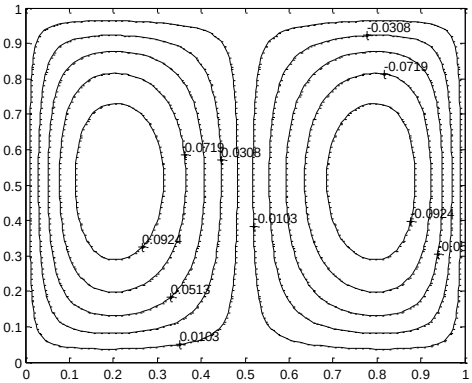

Fig. 11. Streamlines of natural convection in a square cavity for $Ra=10^6$ and $Ha=200$

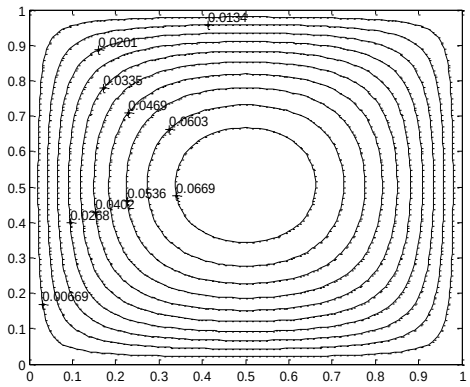

Fig. 12. Isotherms of natural convection in a square cavity for Ra=10^6 and Ha=300

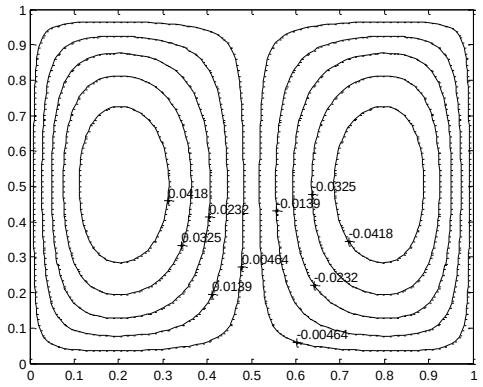

Fig. 13. Streamlines of natural convection in a square cavity for Ra=10^6 and Ha=300

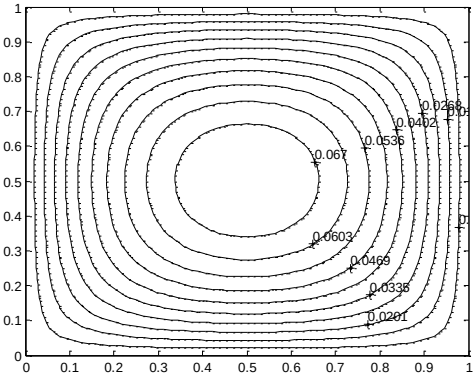

Fig. 14. Isotherms of natural convection in a square cavity for Ra=10^6 and Ha=500

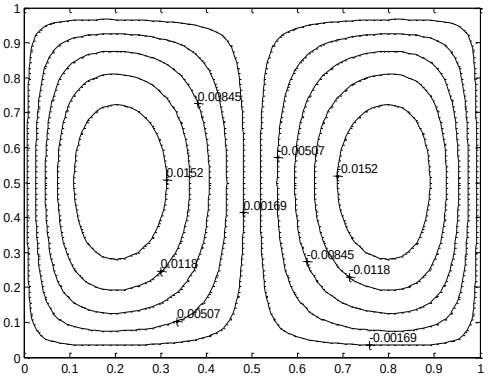

Fig. 15. Streamlines of natural convection in a square cavity for Ra=10^6 and Ha=500

value of stream function is as a measure of the intensity of natural convection in the cavity. It is evident from the table2 that in absent of magnetic field, by increasing the Ra, the maximum value of the stream function increases; this means that the flow move faster as natural convection to be stronger and the isotherm will be distorted.

For the square cavity, the maximum dimensionless temperature (θ_{max}) reduces with increasing Ra. This is because as Ra increases, heat transfer due to convection increases. It is also observed that at low Ra number, the θ_{max} is at the centre of the cavity and it shifts upwards with increase in Ra. For $Ra \geq 5\times10^5$ due to strong convective rolls, two local temperature maxima are observed in the cavity. These maxima shift upwards and towards side walls with the increase in Ra. The fluid circulates in the square cavity as two symmetrical counter-rotating rolls, moving upwards at the center and downwards near the cold side walls.

By applying a magnetic field we can suppress the natural convection so that the maximum value of the stream function reduces as Ha number increases and θ_{max} is at the center of the cavity, indicating that most of the heat transfer is by heat conduction. For high Rayleigh number and for a weak magnetic field strength, convection is dominant heat transfer mechanism. From the streamlines pattern we see that as the Ha number increases, the streamlines will be parallel with the two side walls of the cavity and the streamlines are elongated. On the other hand it is clear from table 2 that for all Ra numbers by increasing the Ha number have a pure conduction regime. Because Lorentz force interacts with the buoyancy force and suppresses the convection flow by reducing the velocities. Furthermore, it is shown that as the Ra number is increased, the convective heat transfer is increased, so that for suppression of convection is needed very high magnetic field.

As it was mentioned, natural convection of electrically conductive fluid in the enclosure is affected by buoyancy and Lorentz forces. The buoyancy force has an aiding effect on natural convection, but the Lorentz force has an opposing effect. Either of the two forces are important, when $Ha^2/Ra \approx 1$. The buoyancy force is dominant when $Ha^2/Ra << 1$ and the Lorentz force is dominant when $Ha^2/Ra >> 1$. Variations of the maximum temperature in terms of Ha^2/Ra for various Ra are shown in Fig. 16. The figure 16 shows that at $Ha^2/Ra > 0.1$, the value of maximum temperature is constant (conduction regime). While at low Ha^2/Ra ($Ha^2/Ra < 0.005$), the electromagnetic body force can be ignored.

Table 2 Variation of θ_{max} and Ψ_{max} with *Ha* and *Ra* numbers

Ra	*Ha*	θ_{max}	Ψ_{max}
10^4	0	0.073407	0.31624
	50	0.073655	0.01594
	100	0.073656	0.0043178
	200	0.073657	0.0011301
	300	0.073657	0.0005104
	500	0.073657	0.0001858
10^5	0	0.064737	2.3075
	50	0.073587	0.15926
	100	0.073645	0.043171
	200	0.073656	0.011301
	300	0.073657	0.0051045
	500	0.073657	0.0018587
10^6	0	0.045875	6.4695
	50	0.068887	1.4913
	100	0.073167	0.42893
	200	0.073622	0.11296
	300	0.073641	0.051033
	500	0.073655	0.018586
10^7	0	---	---
	50	0.044108	6.4406
	100	0.058396	3.3591
	200	0.070802	1.0867
	300	0.072981	0.50574
	500	0.073553	0.18560

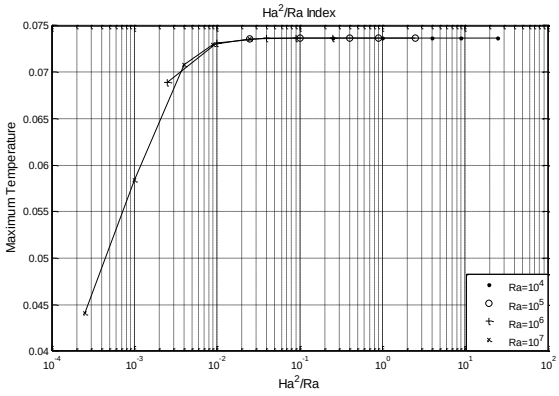

Fig. 16. The maximum temperature versus Ha^2/Ra for various *Ra*

5. CONCLUSION

Author has investigated the laminar steady convection flow in a cavity in the presence of a magnetic field in this paper. The cavity is filled with an electrically conducting fluid whose Prandtl number is 0.733. Author has developed a two-dimensional numerical model to solve the vorticity, stream function and temperature governing equations of buoyancy-driven natural convection flow inside the cavity. The stream function equation is solved using fast Poisson's equation solver on a rectangular grid (POICALC function in MATLAB software), voricity and temperature equations are solved using red-black Gauss-Seidel and bi-conjugate gradient stabilized (BiCGSTAB) methods respectively. The effect of the magnetic field is to reduce the convective heat transfer inside the cavity. Furthermore, when the *Ra* number is increased, the convective heat transfer is increased, so that for suppression of convection is needed very high magnetic field. The ratio of the Lorentz force to the buoyancy force (Ha^2/Ra) is as an index to compare the contribution of natural convection and magnetic field intensity on heat transfer:

a) Thermally driven natural convection exists when $Ha^2/Ra < 0.005$.
b) Electromagnetically driven flows occur when $Ha^2/Ra > 0.1$.
c) Natural convection occur by both electromagnetic body force and gravitational body force when $0.005 < Ha^2/Ra < 0.1$.

REFERENCES

Al-Najem N.M., Khanafer K.M., El-Refaee M.M. (1998); "*Numerical Study of Laminar Natural Convection in Tilted Enclosure with Transverse Magnetic Field*"; Int J Num Method Heat Fluid Flow, 8(6), 651–672.

Bagewadi C.S., Bhagya S. (2011), "*Solutions in Variably Inclined MHD Flows*", Journal of Applied Fluid Mechanic, 4(4), 77-83.

Borghi C.A., Carraro M.R., Cristofolini A. (2004);" *Numerical Solution of the Nonlinear Electrodynamics in MHD Regimes with Magnetic Reynolds Number near One*", IEEE Trans. Magn., 40(2), 593-596.

Borghi C.A., Cristofolini A., Minak G. (1996);" *Numerical Methods for the Solution of the Electrodynamics in Magnetohydrodynamic Flows*", IEEE Trans. Magn. , 32(3), 1010-1013.

Ece M.C., Büyük E. (2006); "*Natural-Convection Flow under a Magnetic Field in an Inclined Rectangular Enclosure Heated and Cooled on Adjacent Wall*", Fluid Dynam. Res., 38, 564–590.

Ece M.C., Büyük E. (2007); "*Natural Convection Flow under a Magnetic Field in an Inclined Square Enclosure Differentialy Heated on Adjacent Walls*", Meccanica, 42, 435–449.

Erturk E. (2009);" *Discussions on Driven Cavity Flow*", Int. J. Num. Meth. Fluids, 60, 275–294.

Garandet J.P., Alboussiere T. (1992);" *Buoyancy Driven Convection in a Rectangular Enclosure with a Transverse Magnetic Field*", Int J Heat Mass Transf, 35(4), 741-748.

Gupta M.M., Kalita J.C. (2005);" *A new paradigm for solving Navier–Stokes equations: stream function–velocity formulation*", J. Comput. Phys., 207, 52–68.

Kadid F.Z., Drid S., Abdessemed R. (2011), "*Simulation of Magnetohydrodynamic and Thermal Coupling in the Linear Induction MHD Pump*", Journal of Applied Fluid Mechanic, 4(1), 51-57.

Kandaswamy P., Sundari S.M., Nithyadevi N. (2008);" *Magnetoconvection in an Enclosure with Partially Active Vertical Walls*", Int J Heat Mass Transf, 51, 1946–1954.

Krzeminski S.K., Smiałek M., Wlodarczyk M. (2000);" *Finite Element Approximation of Biharmonic Mathematical Model for MHD Flow using Ψ-A Approach*", IEEE Trans. Magn., 36(4), 1313-1318.

Mahmud S., Tasnim S.H., Mamun M. A. H. (2003);" *Thermodynamic Analysis of Mixed Convection in a Channel with Transverse Hydromagnetic Effect*", Int. J. Thermal Sci, 42, 731–740.

Piazza I.D., Ciofalo M. (2002);" *MHD Free Convection in a Liquid-Metal Filled Cubic Enclosure. II. Internal Heating*", Int J Heat Mass Transf, 45, 1493–1511.

Pirmohammadi M., Ghassemi M. (2009);" *Numerical Study of Magneto-Convection in a Partitioned Enclosure*", IEEE Trans. Magn, 45(6), 2671- 2674.

Pirmohammadi M., Ghassemi M., Hamedi M. (2010);" *Effect of Inclination Angle on Magneto-Convection Inside a Tilted Enclosure*", IEEE Trans. Magn, 46(9), 3697-3700.

Pirmohammadi M., Ghassemi M., Keshtkar A. (2011); "*Numerical Study of Hydromagnetic Convection of an Electrically Conductive Fluid with Variable Properties Inside an Enclosure*", IEEE Trans. Plasma Sci, 39(1), 516-520.

Pirmohammadi M., Ghassemi M., Sheikhzadeh G.A. (2009); "*Effect of a Magnetic Field on Buoyancy-Driven Convection in Differentially Heated Square Cavity*", IEEE Trans. Magn , 45(1), 407-411.

Salah N.B., Soulaimani A., Habashi W.G. (2001);" *A Finite Element Method for Magnetohydrodynamics*", Comput. Meth. Appl. M., 190, 5867-5892.

Sarris I.E., Kakarantzas S.C., Grecos A.P., Vlachos N.S. (2005); "*MHD Natural Convection in a Laterally and Volumetrically Heated Square Cavity*", Int J Heat Mass Transf, 48, 3443–3453.

Shadid J.N., Pawlowski R.P., Banks J.W., Chacon L., Lin P.T., Tuminaro R.S. (2010);" *Towards a Scalable Fully-Implicit Fully-Coupled Resistive MHD Formulation with Stabilized FE Methods*", J. Comput. Phys., 229, 7649–7671.

Sheikhzadeh G.A., Fattahi A., Mehrabian M.A. (2011); "*Numerical Study of Steady Magneto-Convection around an Adiabatic Body inside a Square Enclosure in Low Prandtl Numbers*", Heat Mass Trans, 47, 27–34.

Sugilal G., Wattal P.K., Iyer K. (2005);" *Convective Behaviour of a Uniformly Joule-Heated Liquid Pool in a Rectangular Cavity*", Int. J. Thermal Sci, 44, 915–925.

Verardi S.L.L, Cardoso J.R. (1998); "*A Solution of Two-Dimensional Magnetohydrodynamic Flow using the Finite Element Method*", IEEE Trans. Magn., 34(5), 3134-3137.

Verardi S.L.L, Cardoso J.R., Costa M.C. (2001);" *Three-Dimensional Finite Element Analysis of MHD Duct Flow by the Penalty Function Formulation*", IEEE Trans. Magn., 37(5), 3384-3387.

Verardi S.L.L, Machado J.M., Cardoso J.R. (2002);" The Element-Free Galerkin Method Applied to the Study of Fully Developed Magnetohydrodynamic Duct Flows", IEEE Trans. Magn., 38(2), 941-944.